# Partitioning of Flight Data for Aerodynamic Modeling of Aircraft at High Angles of Attack

James G. Batterson*
*NASA Langley Research Center, Hampton, Virginia*
and
Vladislav Klein†
*George Washington University, Hampton, Virginia*

**It is sometimes necessary to determine aerodynamic model structure and estimate associated stability and control derivatives for airplanes from flight data that cover a large range of angle of attack or sideslip. One method of dealing with that problem is through data partitioning. The main purpose of this paper is to provide an explanation of a data partitioning procedure and its application, and to discuss both the power and limitations of that procedure for the analysis of large maneuvers of aircraft. The partitioning methodology is shown to provide estimates for coefficients of those regressors that are well excited in the aircraft motion. In particular, primary lateral stability and damping derivatives are identified throughout the maneuver ranges.**

## Nomenclature

| | |
|---|---|
| $b$ | = wing span, m |
| $C_l, C_n$ | = aerodynamic moment coefficient in roll and yaw, respectively |
| $C_Y$ | = aerodynamic sideforce coefficient |
| $p$ | = roll rate (body axes), rad or deg |
| $r$ | = yaw rate (body axes), rad or deg |
| $t$ | = time, s |
| $V$ | = airspeed m/s |
| $x_i$ | = independent variable (regressors) in regression equations |
| $y$ | = dependent variable in regression equations |
| $\alpha$ | = angle of attack, rad or deg |
| $\bar{\alpha}$ | = midpoint angle of attack of a bin, rad or deg |
| $\beta$ | = angle of sideslip, rad or deg |
| $\delta_a$ | = aileron deflection, rad |
| $\delta_c$ | = canard deflection, rad |
| $\delta_h$ | = horizontal tail deflection, rad |
| $\delta_r$ | = rudder deflection, rad |
| $\theta_i$ | = nondimensional stability or control derivatives in regression equations |

## Introduction

In the field of aircraft system identification, parameter estimation methods are usually applied to small maneuvers that are executed by an aircraft about some trim flight condition, and a linear aerodynamic model is assumed. However, it has been shown[1] that even for cases of small perturbations about a trim angle of attack, a nonlinear aerodynamic model may be required when the trim condition is in or near a region of rapidly changing aerodynamic characteristics (e.g., near stall). In other cases where maneuvers involve large variations in angle of attack, sideslip, or control position, a nonlinear aerodynamic model is almost always necessary. Large maneuvers can be categorized as either commanded or unanticipated. For commanded large maneuvers, it is shown in Refs. 1 and 2 that a proper application of system identification methodology can reveal an aerodynamic model that would otherwise require many small maneuvers.

Large, unanticipated maneuvers are possibly of more interest. Here, the aircraft has lost either stability, damping or control effectiveness in a way neither previously known to the pilot nor reflected in the aerodynamic model. To prevent further incidents, the postflight analysis of these large maneuvers should give some good indication of the cause of the unanticipated motion.

In earlier reports,[1-3] the nonlinear aerodynamic model for large maneuvers was represented either by polynomial splines or by extending the linear terms of the Taylor's series expansion of the aerodynamic force and moment coefficients to include higher-order elements. Implicit to the analysis of the large maneuvers and their nonlinearities in the earlier reports was the procedure of binning or partitioning, i.e., the dividing of a maneuver that covers a large range of some variable into several portions, each of which spans a smaller range of that variable. This technique was introduced in an application to real flight data in Ref. 4. The general applicability of the partitioning technique has now become apparent by its successful application to the diverse aircraft types investigated over the past several years. The main purpose of this paper is to provide an explanation of the partitioning procedure and its application and to discuss both the power and limitations of that procedure for the analysis of large maneuvers of aircraft.

The paper will begin with a general discussion of the partitioning technique. Then, applications of partitioning to the analysis of flight data from large maneuvers of four different aircraft will be presented. The aircraft are a single-engine general aviation type, a modern, twin-engine jet fighter, a three-surface, close-coupled, canard, unpowered drop model, and a one-fifth-scale, unpowered, forward-swept wing drop model. Top view line drawings of these aircraft appear in Fig. 1. The paper concludes with a synopsis of the positive and negative aspects of the partitioning methodology.

## Partitioning

To understand the basis for partitioning, let

$$y(t) = f[x_1(t), x_2(t), ..., x_n(t)] \tag{1}$$

Now suppose that for any $t$ we want to eliminate the dependence of $y(t)$ in one of the variables $x_i(t)$, say $x_p(t)$. Then, by

Presented as Paper 87-2621 at the AIAA Atmospheric Flight Mechanics Conference, Monterey, CA, Aug. 17-19, 1987; received Oct. 20, 1987; revision received April 2, 1988. 

*Research Scientist, Aircraft Guidance and Controls Branch. Associate Fellow AIAA.

†Professor of Engineering, Joint Institute for Advancement of Flight Sciences. Associate Fellow AIAA.

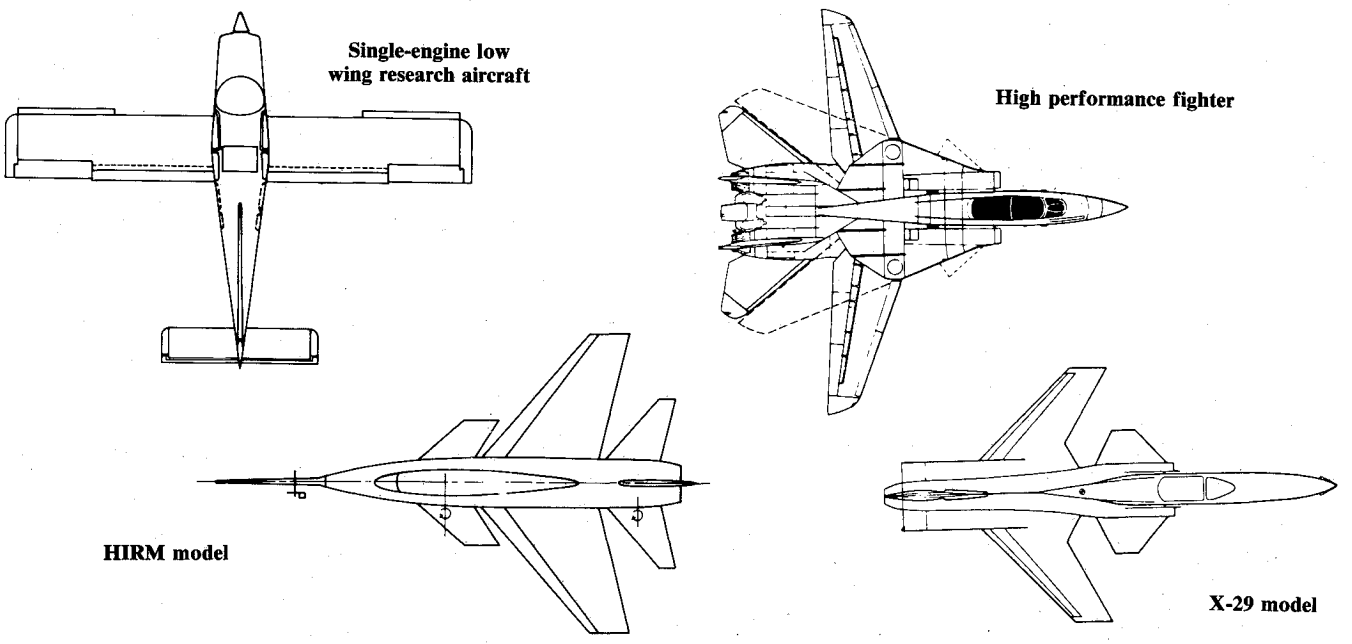


**Fig. 1 Top view line drawing of test aircraft.**

partitioning, we mean redefining $y(t)$ on proper subsets of $\{x_1,x_2,...,x_n\}$ as

$$y(\bar{x}_p,t) = \begin{cases} f_1[x_1(t), x_2(t), ..., x_{p-1}(t), x_{p+1}(t), ..., x_n(t)] \\ \quad \text{for} \quad x_{p0} < x_p < x_{p1} \\ f_2[x_1(t), x_2(t), ..., x_{p-1}(t), x_{p+1}(t), ..., x_n(t)] \\ \quad \text{for} \quad x_{p1} < x_p < x_{p2} \\ \vdots \\ f_m[x_1(t), x_2(t), ..., x_{p-1}(t), x_{p+1}(t), ..., x_n(t)] \\ \quad \text{for} \quad x_{p_{m-1}} < x_p < x_{p_m} \end{cases} \quad (2)$$

where

$$\bar{x}_p = \frac{x_{p_{i+1}} + x_{p_i}}{2}, \qquad i = 1,2,...,m$$

That is, each $n+1$ tuple in $(x_i,y)$ is reduced to several $n$-tuples—each associated with a particular value on a small range of $x_p$. The supposition is that as the range defined by $x_p$ becomes smaller, the variation in $f$ due to $x_p$ can be neglected. For example, an aircraft might perform a mostly lateral maneuver, but with angle of attack $\alpha$ varying between 20 and 30 deg. We could expect that, due to separation effects on the lifting surfaces in this $\alpha$ region, the lateral aerodynamic force and moment coefficients $C_Y$, $C_l$, $C_n$ might well depend on $\alpha$ in a nonlinear way; i.e.,

$$C_n = C_n(\alpha,\beta,p,r,\delta_{\text{control}}) \quad (3)$$

Then, to partition, one would simply analyze the data in separate groupings as follows:

$$\begin{aligned} C_n(\bar{\alpha} = 21 \text{ deg}) &= C_n(\beta,p,r,\delta_{\text{control}})_{20 \text{ deg}} < \alpha < 22 \text{ deg} \\ C_n(\bar{\alpha} = 23 \text{ deg}) &= C_n(\beta,p,r,\delta_{\text{control}})_{22 \text{ deg}} < \alpha < 24 \text{ deg} \\ &\vdots \\ C_n(\bar{\alpha} = 29 \text{ deg}) &= C_n(\beta,p,r,\delta_{\text{control}})_{28 \text{ deg}} < \alpha < 30 \text{ deg} \end{aligned} \quad (4)$$

That is, all data corresponding to 20 deg $< \alpha <$ 22 deg are put into one group for analysis, data corresponding to parts of the maneuver in which 22 deg $< \alpha <$ 24 deg are put into a second group and so forth until all data have been accounted for.

If any grouping still appears to be dependent on $\alpha$, it can be subdivided further, assuming a sufficient number of data points exist. In this example one can now analyze $C_n = f(\beta,p,r,\delta_{\text{control}})$ at characteristic values of $\alpha$ given by the mean value of $\alpha$ for each grouping.

In selecting the data for a subset, the only consideration here is the value of $\alpha$. Therefore, it will quite possibly be the case that the data in a given subset are not all contiguous in time. Several sections of the maneuver will probably be combined. For example (Fig. 2), in partitioning a large maneuver that lasted 20 s, bin 2 contains four noncontiguous time sections of data (all data corresponding to 4 deg $< \alpha <$ 8 deg), viz., the segment from 0–4 s, a segment around 6 s, a segment around 7 s, and a segment around 12.5 s. Moreover, data from several large maneuvers may be combined and the resulting combined set partitioned.

After the bins or subsets are established, the model structure determination and parameter estimation can proceed. The model structure determination is still necessary, since large variations also may have occurred in variables other than the one on which the partitioning is based. The model structure determination and parameter estimation then proceeds by applying a modified stepwise regression (MSR) algorithm[2] to each bin or subset of partitioned data. We will explore MSR further in the next section.

## Modified Stepwise Regression

All of the data from each bin were analyzed using a modified stepwise regression (MSR). As a modified version of the linear regression, this method can determine the structure of aerodynamic model equations and estimate the model parameters. The determination of an adequate model for the aerodynamic coefficients includes three steps: the postulation of terms that might enter the model, the selection of an adequate model, and the verification of the model selected. The general form of aerodynamic model equations can be written as

$$y(t) = \theta_0 + \theta_1 x_1(t) ... + \theta_n x_n(t) \quad (5)$$

where $y(t)$ represents the resultant coefficient of aerodynamic force or moment. In the polynomial representation of the aerodynamic coefficient, $\theta_1,...,\theta_n$ are the stability and control derivatives, $\theta_0$ is the value of any particular coefficient corresponding to the initial steady-flight conditions, and $x_1,...,x_n$ are the regressors formed by the airplane output and control variables or their combinations.

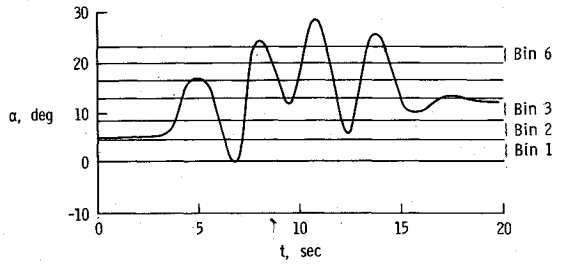


**Fig. 2 Data partitioning for a large-amplitude longitudinal maneuver.**

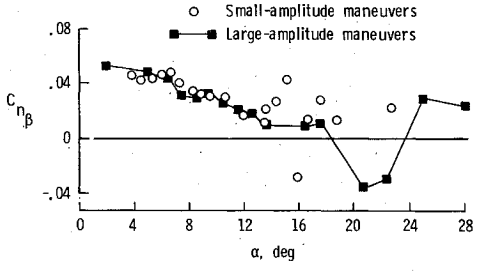


**Fig. 3 Comparison of directional stability parameter estimated from small- and large-amplitude maneuvers with partitioned data.**

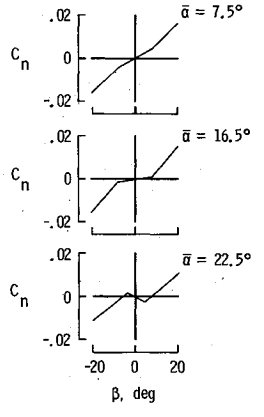


**Fig. 4 Steady-state values of yawing-moment coefficient estimated from large-amplitude maneuvers with partitioned data.**

After postulating the aerodynamic model equations, the determination of significant terms among the candidate variables and estimation of the corresponding parameters follows. The variable chosen for entry into the regression equation is the one that has the largest correlation with $y$ after adjusting for the effect on $y$ of the variables already selected. The parameters are estimated by minimizing the cost function

$$J_{SR} = \sum_{i=1}^{N} \left[ y(i) - \theta_0 - \sum_{j=1}^{l} \theta_j x_j(i) \right]^2 \qquad (6)$$

where $N$ is the number of data points and $(l+1)$ is the number of parameters in the regression equation.

At every step of the regression, the variables incorporated into the model in previous stages and a new variable entering the model are re-examined. Any variable that provides an insignificant contribution (due to correlation with more recently added terms) is removed from the model. The process of selecting and checking variables continues until no more variables are admitted to the equation and no more are rejected. Experience shows, however, that the model based only on the significance of individual parameters in the model in Eq. (6) can still include too many terms and, therefore, may have poor prediction capabilities. Several criteria for the selection of an adequate model are introduced in Ref. 1, and the details of the whole procedure are explained in Refs. 1 and 2.

## Examples

This first example, taken from Refs. 2 and 3, deals with analysis of commanded large maneuvers of a single-engine, low-wing research airplane. The emphasis in this example is on 1) a comparison of the results from partitioning with those achieved with 30 small-amplitude maneuvers, and 2) the capability to discover nonlinearities in a second variable after partitioning with respect to the first. The basic characteristics of the airplane and instrumentation systems are presented in Ref. 5. This airplane had undergone certain wing leading-edge modifications that allowed trimmed flights at angles of attack up to approximately 24 deg. The measured data were available in the form of input and output time histories sampled at 0.05-s intervals. These data comprised two sets of maneuvers. For the first set, 30 small-amplitude lateral maneuvers were excited by control-surface deflections at trimmed conditions within the $\alpha$ range of 2–24 deg. From these maneuvers, local models of aerodynamic coefficients were estimated. The second set of data consisted of large-amplitude combined longitudinal and lateral maneuvers with the $\alpha$ variation between 0 and 30 deg. The combined maneuvers were accomplished by persistent excitation of lateral responses by rudder and aileron doublets superimposed on a steadily increasing angle of attack due to slow but steady increase in elevator deflection. The measurements from 12 combined maneuvers were joined together into one set of data. The resulting ensemble of about 13,000 data points was then partitioned into 22 subsets according to the values of $\alpha$. The modeling of the lateral parameters was conducted mostly on 1 deg subspaces of the 0–30 deg $\alpha$-space. As an example, the model for $C_n$ was postulated as

$$C_n(\bar{\alpha},\beta,p,r,\delta_a,\delta_r) = C_{n_\beta}\beta + \sum_{i=1}^{5} C_{n_{\beta_i}}\beta\left(1 - \frac{\beta_i}{|\beta|}\right) + C_{n_p}pb/2V + C_{n_r}rb/2V + C_{n_{\delta a}}\delta a + C_{n_{\delta r}}\delta r \qquad (7)$$

where

$$\left(1 - \frac{\beta_i}{|\beta|}\right)_+ = \begin{cases} 0 & (|\beta| < \beta_i) \\ \beta - \beta_i & (\beta \geq \beta_i) \\ \beta + \beta_i & (\beta \leq -\beta_i) \end{cases}$$

The knots of spline in $\beta$ were selected at 4, 8, 12, 16, and 20 deg. The estimates of the directional stability parameter $C_{n_\beta}$ from partitioned data are presented in Fig 3. In general, these estimates are consistent with the results from small-amplitude maneuvers. Some differences arise for $\alpha > 13$ deg and continue to $\alpha = 28$ deg. The reason for such a discrepancy might be explained by Fig. 4, in which the nonlinearity of $C_n$ with $\beta$ for $\alpha > 15$ deg is clearly shown. These estimates could not be achieved from the small-amplitude maneuvers and indicate the power of partitioning in achieving an aerodynamic model that is valid over a large range of angle of attack and sideslip.

The second example involves flight data from a twin-engine, high-performance fighter with variable wing sweep.[6] A top view line drawing is given in Fig 1. In this example, we will emphasize comparison with wind-tunnel results and the maneuver dependence of the estimates of the roll damping parameter $C_{l_p}$.

For this airplane, the left and right norizontal stabilator act both symmetrically and differentially, providing pitch and roll control, respectively. The average setting of the stabilator provides the pitch control. At low speeds, spoilers on the wing are used for additional roll control. The rudders on the twin vertical tails provide control in yaw. The test configuration consisted of the wing in the 21-deg sweep position with full-span slats on the outboard panels deflected at 8.5 deg and the trailing-edge flap deflected at 11 deg.

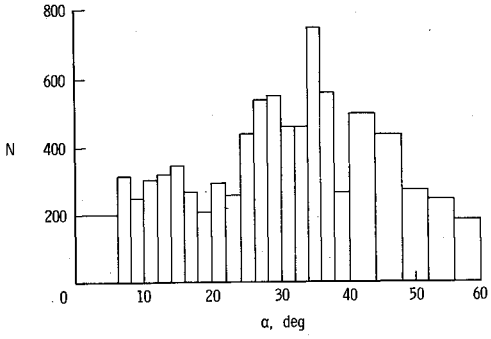


**Fig. 5 Number of data points in subsets using partitioning of data from large-amplitude maneuvers.**

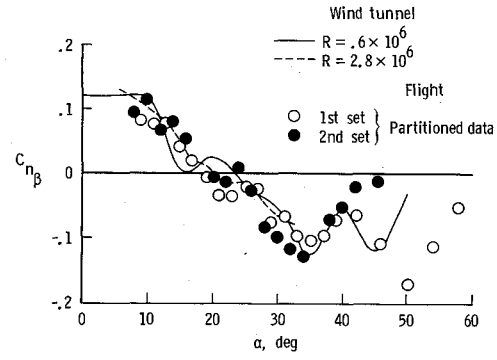


**Fig. 6 Comparison of directional stability parameter estimated from large-amplitude maneuvers and wind-tunnel measurement.**

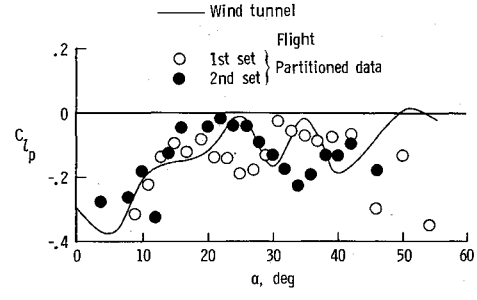


**Fig. 7 Comparison of damping-in-roll parameter estimated from large-amplitude maneuvers and wind-tunnel measurement.**

The flight data were obtained in the form of input-output time histories with 50 samples/s. The data available for the analysis included two sets of large-amplitude transient maneuvers. The first set was not intended for model structure determination and parameter estimation. The maneuvers were flown for the evaluation of stability and handling characteristics in high $\alpha$ flight regimes. In these maneuvers, the motion consisted of predominantly lateral modes, with $\alpha$ changing from 0 to 60 deg and $\beta$ sometimes exceeding 25 deg. The time histories indicated that the large-amplitude maneuvers contained some possible deficiencies for use in airplane parameter identification. For example, during these maneuvers, all airplane modes were not persistently excited because of the small variation in the differential tail and rudder deflection. Very often, the maneuvers started with rapid changes in $\alpha$, $\theta$, and $V$ but only small variations in the remaining output variables. For these reasons, the data from 19 maneuvers were joined together into one set of data. The resulting ensemble of about 9000 data points was partitioned into 23 subsets according to the values of $\alpha$. A histogram summarizing the number of data points in each subset is given in Fig. 5, where the width of each rectangle represents the width of the corresponding subset and the height corresponds to the number of points in that subset. For the new sets of data, the lateral coefficients were modeled primarily on 2-deg subspaces of the 0–60 deg $\alpha$-space.

In contrast to the first set of large-amplitude maneuvers, the second set was flown explicitly for parameter estimation. This second set of large-amplitude data comprised four combined (longitudinal and lateral) transient maneuvers. The four combined maneuvers were joined and the resulting data set was partitioned into 2-deg subspaces of the 0–50 deg $\alpha$-space.

The estimates of the directional stability parameter $C_{n_\beta}$ from the two sets of large maneuvers are given in Fig. 6 along with published results from low- and high-Reynolds-number wind-tunnel tests. These estimates correspond to $\beta$ between $\pm 5$ deg and are referred to $\delta_h = 0$ deg. The effect of different test conditions on wind-tunnel values is also seen in Fig. 6. The estimates from large-amplitude maneuvers agree reasonably well with the wind-tunnel data for $10 \text{ deg} < \alpha < 40$ deg. The scatter in the estimates for $\alpha > 40$ deg can be caused by dynamically induced separation effects in poststall flight conditions.

The dependence of parameter estimates on the dynamics of the maneuver is seen in the values of damping-in-roll parameter $C_{l_p}$, which are plotted vs $\alpha$ in Fig. 7. The results from the two sets of partitioned data exhibit some inconsistency for $\alpha > 20$ deg. This could be caused by different flight conditions and types of maneuvers. The first set of data included various maneuvers with the rolling velocity sometimes reaching 100 deg/s. The maneuvers included in the second set of partitioned data were mostly oscillatory, with rolling velocity within the $\pm 30$ deg/s range. Since the flight estimates and the wind-tunnel results only show partial agreement, one might examine more closely the roll damping in the $\alpha = 25$ and 35 deg regions through additional tests.

The third example is for the high incidence research model (HIRM). The HIRM was designed, built, and flown by the Royal Aircraft Establishment (RAE), Farnborough, England, for the purpose of research on flight dynamics and departure prevention at high angles of attack.[7] This example will illustrate how partitioning data from several unanticipated, large lateral oscillations along with the analysis of individual maneuvers can produce estimates of the damping derivative $C_{l_p}$ that were not achieved by either oscillatory or rotary wind-tunnel tests. Also, the sensitivity of the model to canard setting will be shown.

The HIRM is a three-surface, unpowered model with an advanced transonic swept wing, an all-moving canard and stabilator, and an oversized vertical tail with rudder. The wing has no moving control surfaces. Roll control is provided by differential canard and stabilator deflection. The general arrangement of the model is shown in Fig. 1. The model is fully instrumented with the transducer signals telemetered to a ground station. Flight maneuvers are preprogrammed into the system and executed by a timer after the model is released from a carrier helicopter. The duration of the flights varied between 80 and 160 s.

The motion of the HIRM was initially excited by the model's release from the helicopter cable and then by the activation of control surfaces. For each test run, either doublet in differential tail or canard, or simple rudder pulses were used. In some maneuvers, a step deflection of symmetric tail was added. The various trim conditions were established by the canard setting at either 0 or $-10$ deg and by the tailplane setting between $-14$ and $-20$ deg. Most of the responses were within the $\alpha$-range of 20–40 deg, though in three maneuvers $\alpha$ reached 60 deg.

The measured data from five flights with 26 maneuvers were obtained as time histories of control and response variables sampled at 0.012-s intervals. The two flights with $\delta_c \doteq -10$ deg and $\delta_h \doteq -18$ deg are designated as HD1 and HD3, the remaining three flights with $\delta_c \doteq 0$ deg and $\delta_h \doteq -15$ deg as HD2, HD4 and HD6.

In addition to analyzing almost all of the 26 individual maneuvers, the data from each flight were joined together into

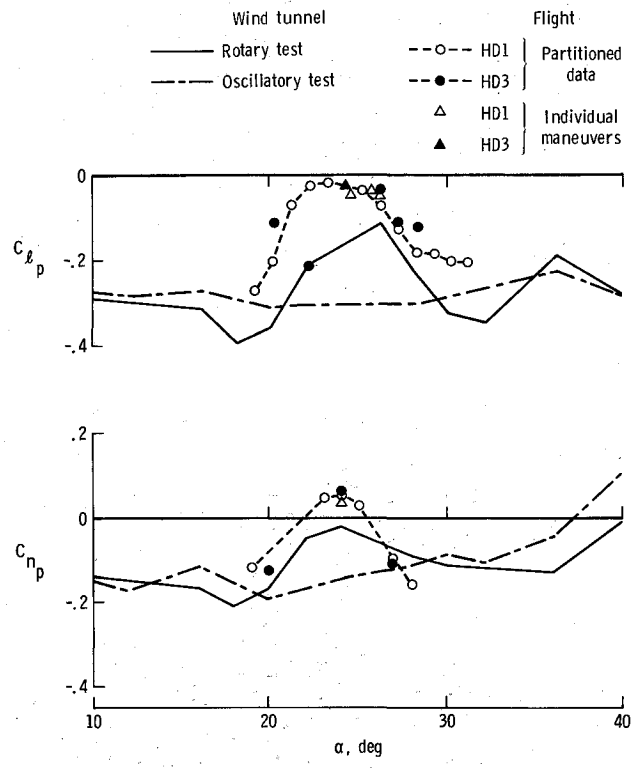


**Fig. 8 Comparison of oscillatory roll-rate parameters estimated from flight data and wind-tunnel measurement.**

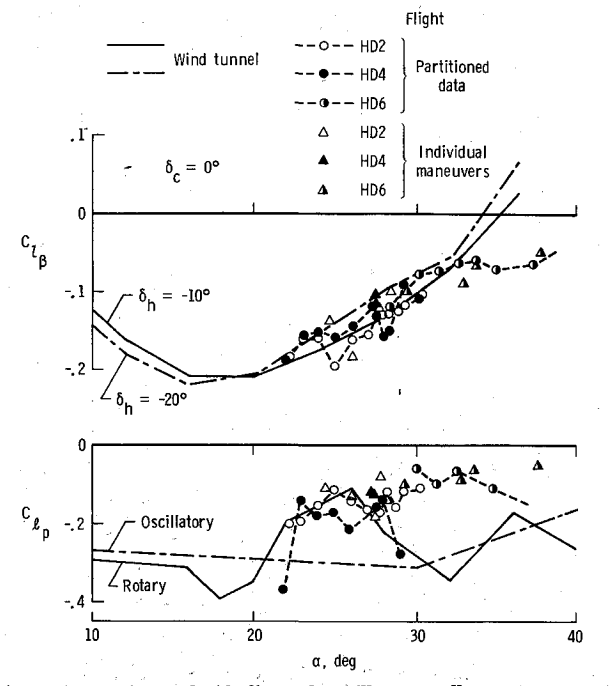


**Fig. 9 Comparison of sideslip and oscillatory roll-rate parameters estimated from flight data and wind-tunnel measurement.**

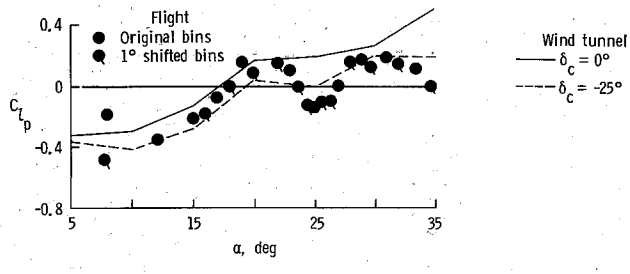


**Fig. 10 Comparison of damping-in-roll parameter estimated from partitioned flight data and wind-tunnel measurement.**

one set of data. The resulting ensemble was then partitioned into subsets according to the value of $\alpha$. For these new subsets of data, the aerodynamic coefficients were modeled mostly on 1-deg subspaces of the original $\alpha$-space.

In Fig. 8, $C_{l_p}$ and cross-derivative $C_{n_p}$ are compared with the results from the oscillatory and rotary wind-tunnel tests. The rotary data predicted a decrease in damping for 20 deg $< \alpha <$ 28 deg, whereas the oscillatory tests show no deterioration in this region. The flight data indicate even less damping-in-roll than the rotary test. The flight results are in agreement with the observed responses of the drop model, which show very little damping or no damping at all. The reason for the discrepancy between the oscillatory data and flight results can be due to the different amplitude or oscillation in the wind-tunnel ($\pm 5$ deg) and in flight (around $\pm 35$ deg). The comparison of $C_{n_p}$ parameters from various tests shows a similar pattern to that of $C_{l_p}$. No nonzero estimates of $C_{n_p}$ could be obtained from the partitioned data for 19 deg $< \alpha <$ 23 deg.

The effect of different canard setting is shown in two examples, where $\delta_c = 0$ deg and $\delta_h = -18$ deg. In the upper part of Fig. 9, the parameter estimates of $C_{l_\beta}$ from flights HD2, HD4 and HD6 are plotted and compared with wind-tunnel data for $\delta_h = -20$ deg and $\delta_h = -10$ deg. The consistency of the flight estimates is good, and they agree with the wind-tunnel data for $\alpha < 32$ deg. For higher $\alpha$, the flight results still exhibit negative values for $C_{l_p}$, but the wind-tunnel measurements predict zero and positive dihedral effect. To confirm these differences, more flight data would be needed for $\alpha > 32$ deg. The lower part of Fig. 9 contains the damping parameter $C_{l_p}$ from flight and wind-tunnel testing. The rotary test results agree with flight data for 22 deg $< \alpha <$ 27 deg. For the $\alpha$-region between 27 and 35 deg, the flight data still indicate low damping in roll, which is not confirmed by wind-tunnel measurements. A comparison of flight results in Figs. 8 and 9 indicates the strong effect of canard setting on damping in roll.

The final example is the analysis of an apparent wing rock event of a 22% scale forward-swept-wing, free-flight drop model. This example[8] illustrates the use of partitioning for the estimation of stability derivatives to corroborate previous wind-tunnel results early in a flight test program, even though the maneuvers were not intended for parameter estimation. The data were recorded during the first two flights of the test vehicle, before the ground-based pilot was familiar with the aircraft flight responses. Wind-tunnel testing had indicated a potential for wing rock for angles of attack greater than 20 deg.[9] The potential source of the wing rock was a loss of roll damping as reflected in $C_{l_p}$, which became positive for $\alpha > 20$ deg. Indeed, wing rock did develop in flight and the model was very difficult to control for $\alpha > 20$ deg. To either confirm or refute the loss of roll damping as a cause, the partitioning methodology was applied to the recorded flight data. Though no control effectiveness derivatives could be estimated, all primary lateral stability derivatives $C_{Y_\beta}$, $C_{l_\beta}$, $C_{n_\beta}$ were estimated, as was $C_{l_p}$.

The test vehicle was a 22% dynamically scaled unpowered drop model of the X-29 forward-swept-wing aircraft and is shown from the top in Fig. 1. The model was flown 26% statically unstable in pitch and was stabilized using a stability augmentation system commanded from the remote ground station. The vehicle was lifted by helicopter above the Plum Tree Island Test Facility at NASA Langley Research Center and released at an altitude of approximately 6000 ft. The craft was then guided and maneuvered by a pilot at a ground station. The pilot had ground track information, angle of attack, and a long-range camera view of the model available to him. The pilot inputs were telemetered to the test vehicle, and the vehicle air data, responses, and control surface dis-

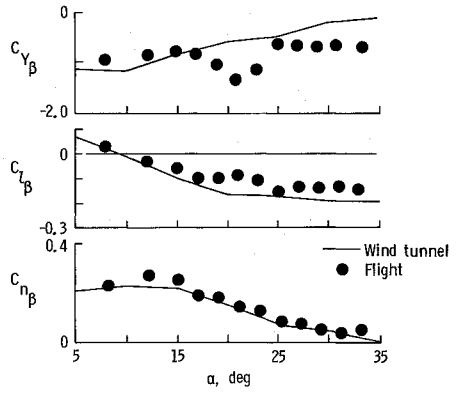


**Fig. 11 Comparison of sideslip parameters estimated from partitioned flight data and wind-tunnel measurement.**

placements were telemetered to the ground station and recorded. The flight data were digitized at 100 samples/s for analysis.

The "standard" maneuver for aircraft system identification consists of trimming the airplane at some specific flight condition and then perturbing the vehicle temporarily from that trimmed condition. By carefully selecting control inputs, excitations and good information content of only the desired modes can result. Because of the pilot's lack of familiarity with the vehicle and the necessity for almost constant turning of the vehicle to keep it within the flight test area, such standard maneuvers were not possible. The pilot did maneuver the craft into the $\alpha > 20$ deg regime three times. The first time led to a violent wing rock followed by a pitch up to $\alpha = 60$ deg and a snap roll; the next two times led to large-amplitude wing rock, but the pilot managed to decrease the vehicle's angle of attack to less than 20 deg to maintain control of the vehicle. In summary, the available flight data from these early flights were not of the quality generally expected for system identification.

Three segments of data comprising approximately 10 s each were combined and partitioned into 2-deg subspaces for $15 \text{ deg} \leq \alpha < 35$ deg and 5-deg subspaces for $5 \text{ deg} \leq \alpha < 15$ deg. The data in these bins were analyzed using the MSR algorithm. Then the boundaries of each bin were shifted up 1 deg in angle of attack and analyzed again using the MSR algorithm. The resulting estimates of $C_{l_p}$ are given in Fig. 10. The flight estimates are compared with wind-tunnel results of canard settings of $-25$ and 0 deg. Canard position in flight varied mainly between $-5$ and $-20$ deg. The flight data indicate, in agreement with the wind tunnel, that roll damping is lost close to $\alpha = 19$ deg. However, the flight data also indicate that roll damping is re-established for $25 \text{ deg} \leq \alpha \leq 27$ deg, while the wind tunnel indicates a continued loss of damping. Both flight and tunnel data then show a loss of roll damping for $\alpha > 27$ deg. The stability derivatives $C_{Y_\beta}$, $C_{l_\beta}$, $C_{n_\beta}$ agreed well with wind-tunnel results (Fig. 11). It was concluded that further investigation of the $25 \text{ deg} < \alpha < 27$ deg region be undertaken.

## Concluding Remarks

Though not a replacement for traditional airplane system identification methodology, data partitioning, followed by application of a stepwise regression algorithm for model structure determination and parameter estimation, has proven to be an effective technique for a first analysis of large maneuvers for diverse types of aircraft. In this paper, the partitioning methodology was shown to provide estimates for coefficients of those regressors that are well excited in the aircraft motion. In particular, primary lateral stability and damping derivatives were identified throughout the maneuver ranges. The combining of data from several maneuvers at similar flight conditions leads to a richer set of points for data analysis. By partitioning with respect to one variable, say $\alpha$, nonlinearities in a second variable, e.g., $\beta$, can be identified. The most consistent problem with employing the partitioning methodology for maneuvers not meant for system identification was an inability to estimate control derivatives. This was probably due to the lack of persistent control surface activity during such maneuvers. In cases of unanticipated aircraft motion, partitioning can provide insight into the cause of the motion and indicate flight regions for further research.

## References

[1]Batterson, J. G., "Estimation of Airplane Stability and Control Derivatives from Large-Amplitude Longitudinal Maneuvers," NASA TM-83185, Oct. 1981.

[2]Klein, V., Batterson, J. G., and Murphy, P. C., "Determination of Airplane Model Structure from Flight Data by Using Modified Stepwise Regression," NASA TP-1916, Oct. 1981.

[3]Klein, V. and Batterson J. G., "Application of Polynomial Splines and Stepwise Regression in the Determination of Airplane Model Structure from Flight Data," NASA TP-2126, March 1983.

[4]Stalford, H. L., "Application of the Estimation-Before-Modeling (EBM) System Identification Method to the High Angle of Attack/Sideslip Flight of the T-2C Jet Trainer Aircraft. Volume III—Identification of T-2C Aerodynamic Stability and Control Characteristics from Actual Flight Test Data," Rept. NADC-76097-30, April 1979.

[5]Klein, V., "Determination of Stability and Control Parameters of a Light Airplane from Flight Data Using Two Estimation Methods," NASA TP-1306, March 1979.

[6]Klein, V. and Batterson, J. C., "Aerodynamic Parameters Estimated from Flight and Wind Tunnel Data," *Journal of Aircraft*, Vol. 23, April 1986, pp. 306–312.

[7]Klein, V. and Mayo, M. H., "Estimation of Aerodynamic Parameters from Flight Data of a High Incidence Research Model," ICAS Paper 86-5.5.2, Sept. 1986.

[8]Raney, D., "Analysis of Lateral Stability for X-29 Drop Model Using System Identification Methodology," AIAA Paper 87-2625-CP, Aug. 1987.

[9]Murri, D. G., Nguyen, L. T., and Grafton, S. B., "Wind-Tunnel Free-Flight Investigation of a Model of a Forward-Swept-Wing Fighter Configuration," NASA TP-2230, Feb. 1984.